International Journal of Concrete Structures and Materials

RESEARCH

Open Access

Strength Development and Neutralization Progress in High-Performance Blended Cement Concrete Exposed to Atmospheric, Tidal, and Submerged Sea Conditions

Hyeong-Ki Kim[1], Jong-Suk Lee[2], Hyeon-Woo Lee[3] and Seung-Jun Kwon[3*]

Abstract

This study investigates the strength development and neutralization depth of high-performance concrete exposed to marine conditions for 7 years on the East coast of South Korea. Blended cements, common in coastal structures, were used. OPC and slag cement showed advantages in strength development, while high-volume fly ash concrete exhibited a disadvantage, especially in external exposure conditions. Despite exposure differences, all mixtures demonstrated a substantial strength increase at 7 years compared to the 28-day period. Models, initially validated for normal-strength concrete, proved effective in predicting long-term behavior. Neutralization depth remained consistent across exposure conditions, with slag cement showing resilience, while fly ash increased depth. Considerations for marine concrete design and construction are discussed.

Highlights

- OPC and slag cement excel in marine strength, while fly ash concrete lags in external exposure.
- Models validated for normal strength prove effective for long-term predictions in seawater.
- Neutralization depth remains consistent across exposure conditions, revealing slag cement resilience.
- High-volume fly ash concrete displays potential strength variations in mass structures near seawater.
- Considerations for marine concrete design and construction are emphasized based on empirical results.

Keywords High-performance concrete, Exposure condition, Seawater, Neutralization, Strength development, Code

Journal information: ISSN 1976-0485 / eISSN 2234-1315

*Correspondence:
Seung-Jun Kwon
jjuni98@hannam.ac.kr
Full list of author information is available at the end of the article

1 Introduction

The compressive strength development in concrete is one of the most fundamental performances for carrying external loads, so that many researches on this characteristic have been performed for a long time (Washa & Wendt, 1975). In a standard curing condition, i.e., immerging in normal water, concrete strength continues to increase with curing periods, but the strength variation is very large depending on the its exposure conditions (Thomas & Matthews, 2004; Washa & Wendt, 1975; Washa et al., 1989). Many models on strength development of concrete have been proposed and widely adopted for quality control of in situ concrete. Several international codes like ACI, *fib*, KCI, and JSCE have been proposed the models on time-dependent compressive strength development, which could be used for early- and latent-ages of concrete (Escalante et al., 2001; Müller et al., 2013; Mun et al., 2014). However, these models only can cover the standard curing condition, but additional validation on the effect of exposure condition for these models is required (Chidiac et al., 2013; Hwang et al., 2004; Kim et al., 1998; Lee et al., 2016; Wang & Park, 2015).

In coastal areas, the distinct exposure environments for concrete can be classified into three groups in terms of durability: the submerged zone, tidal zone, and atmospheric zone (Kwon & Na, 2011). Even with the same concrete mix, strength development may differ based on these conditions (Al-Khaiat & Fattuhi, 2001; Escalante et al., 2001; Jang et al., 2017; Mun et al., 2014; Park et al., 2012). While numerous studies have been published on the durability of coastal concrete, surprisingly few have investigated strength development.

Moreover, there are limited reported cases of concrete neutralization in the submerged, tidal, and atmospheric zones (Saeki, 1991). This scarcity is attributed to the fact that reinforcing steel corrosion is primarily caused by chloride ion penetration rather than neutralization (Zhu et al., 2016). However, chloride ion penetration is known to occur simultaneously with surface neutralization (Weerdt et al., 2014). Therefore, a better understanding of this process is essential for the durability-based design of concrete structures.

Neutralization in the cement matrix of concrete in coastal areas is influenced by two factors: carbonation and sulfate penetration (Liu et al., 2018; Weerdt et al., 2014). First, carbonation can be caused not only by carbon dioxide (CO_2) in the atmosphere, but also by carbonate dissolved in water (Kwon & Na, 2011). In the atmospheric zone, where pores are relatively dry, CO_2 diffuses through the cement matrix pores. In the tidal and submerged zones, where specimens are generally saturated, the possibility of carbonation due to carbonate (CO_3^{2-}) dissolved in seawater may not be ignored. Our previous research confirmed a significant difference in carbonation between specimens immersed in water and sealed to prevent CO_2 dissolution into the water, and those where the water-containing specimen was exposed to the air (Alemu et al., 2022). This carbonation aids in chloride diffusion, as it decomposes C–S–H and Friedel's salt—both hydrates that bind chloride ions—leading to the re-diffusion of chloride (Zhu et al., 2016).

Second, sulfate penetration can occur not only when concrete is submerged in seawater, but also when sulfate (SO_4^{2-}) dissolves in seawater and becomes airborne (Ragab et al., 2016). Although this does not induce delayed ettringite formation (DEF) due to the relatively low concentration of sulfate ions in seawater, it does lower the pH of the cement matrix (Mehta & Haynes, 1975). While research on sulfate attack primarily targets concrete on land with high sulfate concentrations (Liu et al., 2022), there are limited reported cases of concrete neutralization due to sulfate dissolved in seawater (Liu et al., 2018; Ragab et al., 2016; Whittaker, 2014).

This study aims to experimentally confirm the strength development and neutralization depth of high-performance concrete exposed to the submerged zone, tidal zone, and atmospheric zone for 7 years on the East coast of South Korea. Blended cements, primarily used for coastal mass concrete structures, were employed in the study. Compressive strengths of the concrete under standard curing conditions and those exposed to the marine environment were measured and compared with standard models for concrete strength development. Additionally, the neutralization depth of concrete exposed to the three conditions was measured using a phenolphthalein solution and compared with the carbonation depth predicted from the relevant codes (Helland, 2013). Based on the experimental results, considerations for the design and construction of marine concrete structures were discussed.

2 Materials and Mix Proportions

Type I Ordinary Portland Cement (OPC), Grade 100 ground granulated blast furnace slag (GGBFS), and Class F fly ash (FA) were used as binders for high-performance concrete. These materials are standard, and their chemical composition and physical properties are detailed in Table 1. All materials met the specifications of ASTM C 150, C 989, and C 618, respectively.

Natural fine and coarse aggregates were also employed, and their physical properties are presented in Table 2.

The mix proportions are detailed in Table 3, with water-to-binder ratios (w/b) of 0.37, 0.42, and 0.47 employed. Typically, a w/b of 0.47 is used for normal-strength concrete, while 0.42 and 0.37 are common for

Table 1 Chemical properties of OPC, GGBFS, FA

Items	Chemical composition (mass %)							Physical properties	
Types	SiO_2	Al_2O_3	Fe_2O_3	CaO	MgO	SO_3	Ig.loss	Specific gravity (g/cm^3)	Blaine (cm^2/g)
OPC	21.9	5.2	3.4	63.4	2.1	1.9	0.7	3.16	3,214
GGBFS	32.7	13.2	0.4	44.1	5.6	1.8	0.2	2.89	4,340
FA	55.6	27.7	7.0	2.7	1.1	0.4	4.3	2.19	3,621

Table 2 Physical properties of aggregates

Items	G_{max} (mm)	Specific gravity (g/cm^3)	Absorption (%)	F.M
Fine aggregate	–	2.58	1.01	2.90
Coarse aggregate	25	2.64	0.82	6.87

high-performance concrete. GGBFS contents of 30% and 50% per binder were utilized. The 30% is standard for general concrete structures, whereas the 50% is applied for mass concrete, particularly where lower heat generation is desirable. The FA was used at 30% and 50% per binder, ratios significantly higher than typical applications. This mixture is tailored for low-heat mass concrete in marine foundations. A small amount of superplasticizer was incorporated in all mixes to ensure adequate workability, especially at lower water-to-binder ratios, which has the level of 0.9–1.5% of binder weight. The amount of AE admixture was 0.013–0.025% of binder weight.

3 Exposure Conditions for Test and Measurement

Fig. 1 presents photographs of the test site and specimens installed under various marine exposure conditions. The experimental program was conducted over a 7-year period from 2013 to 2020 at an artificial marine exposure site covering approximately 660 m^2. The site was selected based on a tidal variation of approximately 2 m. Three distinct exposure zones were established: atmospheric, tidal, and submerged. The atmospheric zone was located approximately 2–3 m above the high tide level and 10–20 m inland from the shoreline, designed to capture the effects of airborne chloride without direct seawater contact. To reduce the influence of land-borne contaminants, wind-blocking structures were installed along the shoreward side. In the tidal zone, specimens were exposed alternately to air and seawater. They were placed above sea level during high tide and fully submerged during low tide. A protective concrete wall was constructed

Table 3 Mix proportions for test

Name	w/b	Unit weight (kg/m^3)					
		W	OPC	FA	GGBFS	Fine aggregate	Coarse aggregate
OPC-37	0.37	173	467	0	0	790	980
OPC-42	0.42		412	0	0	810	1005
OPC-47	0.47		368	0	0	864	990
GGBFS 30-37	0.37		327	0	140	785	974
GGBFS 30-42	0.42		288	0	124	806	1001
GGBFS 30-47	0.47		258	0	110	860	985
GGBFS 50-37	0.37		234	0	234	782	971
GGBFS 50-42	0.42		206	0	206	803	997
GGBFS 50-47	0.47		192	0	192	892	914
FA30-37	0.37		324	139	0	759	970
FA30-42	0.42		288	124	0	790	981
FA30-47	0.47		258	110	0	845	968
FA50-37	0.37		236	236	0	688	987
FA50-42	0.42		208	208	0	712	1020
FA50-47	0.47		185	186	0	730	1047

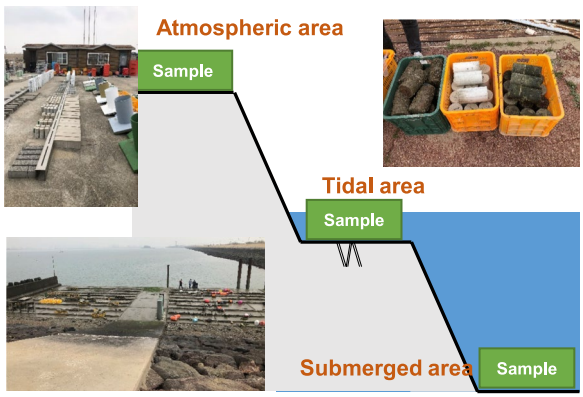

Fig. 1 Conceptual diagram and photographs of the marine exposure site, showing the installation locations of concrete specimens under atmospheric, tidal, and submerged conditions

to limit direct splash impact on the specimens. In the submerged zone, specimens were continuously immersed in seawater, installed within 1 m below the low-tide level, ensuring full and consistent submersion throughout the testing period.

Through field assessments, the chloride ion concentration in seawater was measured within the range of 3.0 to 3.3%, and the air's practical salinity unit (psu) ranged from 25 to 82. Exterior conditions over the last 10 years, including temperature and relative humidity of air, are summarized in Fig. 2. Additionally, the concentration of CO_2 and pH in seawater were also recorded. The atmospheric CO_2 concentration was determined to be in the range of 400 to 420 ppm, while in the seawater, the CO_2 concentration fluctuated between 340 and 470 μatm. The pH of seawater remained stable at a level of 8.0 to 8.1 without significant changes. The results from ten measurements taken between April 2015 and October 2018 are plotted in Fig. 3. The sulfate concentration in the seawater was not directly measured in the present work, but it was reported that within a range from 2.6 to 3.2 mg/L (Kim et al., 2014).

Cylinder specimens with 100×200 mm, cast from ready-mixed concrete, underwent an initial 28-day curing period in water under standard conditions (20 °C) before being placed at the test site. Compressive strength was measured using three or more specimens for each condition according to the designated schedule. Phenolphthalein solution was applied to split cylinder specimens to measure the neutralization depth. During measurement, the entire surface of each specimen was assessed and averaged; this value for each specimen was then averaged again across the three specimens to obtain a single value.

The neutralization depth was measured on the same specimens used for compressive strength testing. The evaluation was conducted in accordance with the Korean Standard (KS) F 2596, which specifies the procedure for assessing carbonation depth in hardened concrete. A phenolphthalein indicator solution was prepared by dissolving 1 g of phenolphthalein in 90 mL of 95% ethanol and then diluting the mixture with distilled water to a total volume of 100 mL, as stipulated in the standard.

4 Codes on Strength Development

The model equations for strength development in standard codes are summarized in Table 4. Typically, these models have parameters that are determined

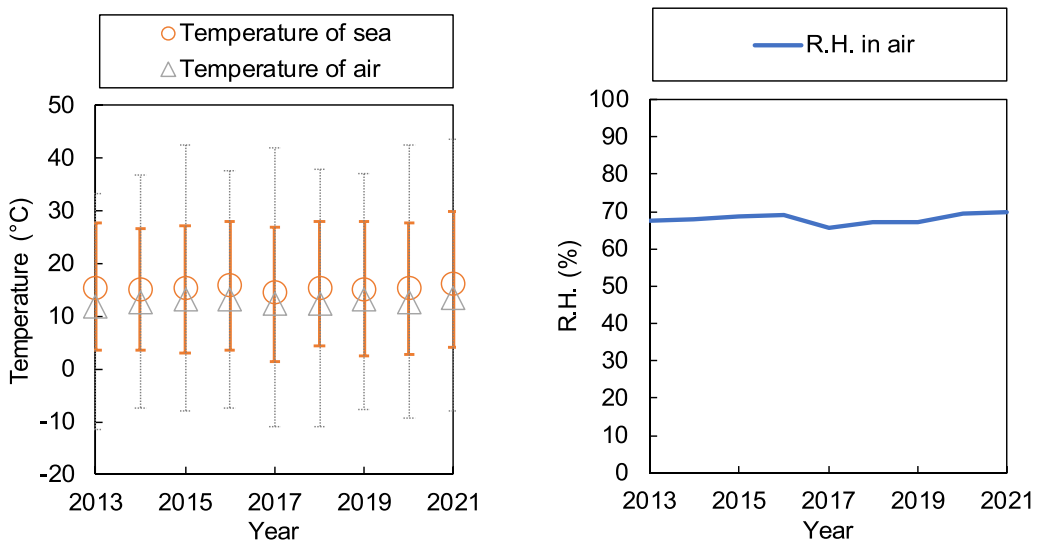

Fig. 2 Temperature and relative humidity data at the site from 2013 to 2021

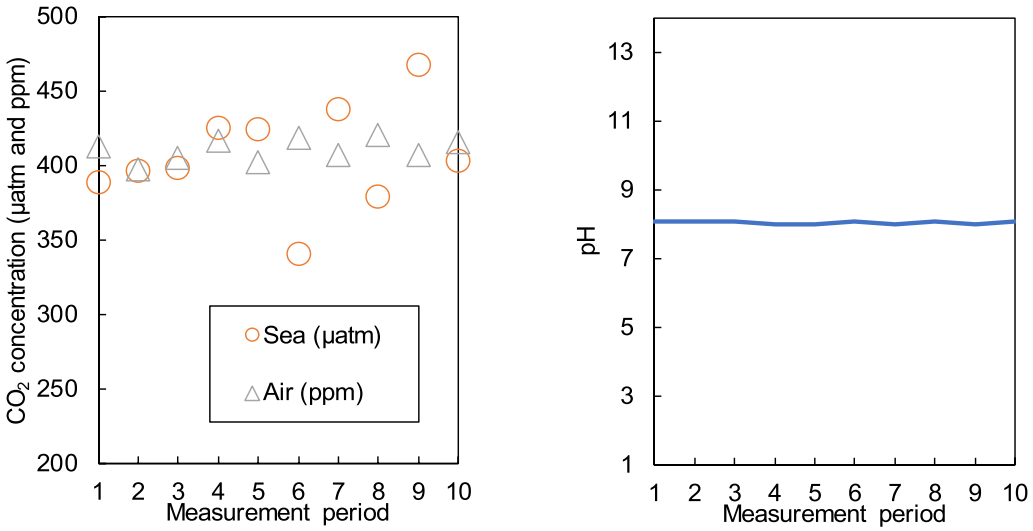

Fig. 3 CO_2 concentration in the air and sea, and pH at the site from 2015 to 2018

Table 4 Models on strength development in the standard codes

Code	Equation	Parameters
KDS 14 20 10	$f_c(t) = \beta_{cc}(t) f_{c28}$, $\beta_{cc}(t) = \exp\left[\beta_{sc}\left(1-\sqrt{\frac{28}{t}}\right)\right]$	β_{sc}: Type I Ordinary Portland Cement: Wet condition 0.35, Steam condition 0.15; High Early Strength Portland Cement: 0.25, 0.12; Moderate Heat Portland Cement: 0.4
ACI 209R [14]	$f_c(t) = \frac{t}{a+bt} f_{c28}$,	Type of cement: Ordinary Portland Cement: Moist-cured concrete a 4.0, b 0.85; Steam-cured concrete a 1.0, b 0.95; High Eary Strength Portland Cement: Moist-cured concrete a 2.3, b 0.92; Steam-cured concrete a 0.7, b 0.98
fib Model Code (MC2010) [4]	$f_c(t) = \beta_{cc}(t) f_{c28}$, $\beta_{cc}(t) = \exp\left[s\left(1-\sqrt{\frac{28}{t}}\right)\right]$	Strength class of cement: 32.5 N; 32.5 R 42.5 N; 42.5 R 52.5 N 52.5 R; s: 0.38; 0.25; 0.20

f_{c28} is the compressive strength at 28 days

based on the type of cement used. However, in the literature, various analytical models for the strength development of concrete have been proposed. These models feature parameters that are sensitive to factors such as the type and content of admixtures, binder characteristics, and curing temperatures.

In this study, the parameters corresponding to Type I Ordinary Portland Cement (OPC) from the standard codes were employed for all models. This choice was made to facilitate a direct comparison with experimental results, as opposed to proposing new parameters for each mixture. Despite the incorporation of a high volume

of mineral admixtures in the cement, the unit weight of OPC in mixtures with low w/b remained within a similar range to that of normal-strength concrete.

5 Results and Discussion

5.1 Compressive Strength

The compressive strength results at 7 years of age for concrete exposed to various conditions are presented in Fig. 4. For comparison, the strength of the 28-day standard-cured specimen is also plotted. For all compressive strength measurements, three or more specimens were tested, and the coefficient of variation was controlled within 15%. While individual standard deviation values or error bars were not included in the figures to maintain readability, the data variation was consistently within acceptable limits. To analyze trends for each condition, Fig. 5 illustrates the ratio of compressive strength for specimens cured under various exposure conditions for 7 years to that of standard-cured specimens with the same duration.

Key observations from Fig. 4 are as follows: first, in the case of mixtures with 30% and 50% GGBFS, and 30% FA, the strength at 7 years was in the same range as the OPC 100% mix, regardless of the exposure condition. However, for the 50% FA mixture, the strength was measured to be higher than OPC under standard curing conditions ('wet curing (7 y)'), but the strength did not develop under external exposure conditions. Nonetheless, for all mixes, a significant increase in compressive strength at 7 years was confirmed compared to the 28-day mix.

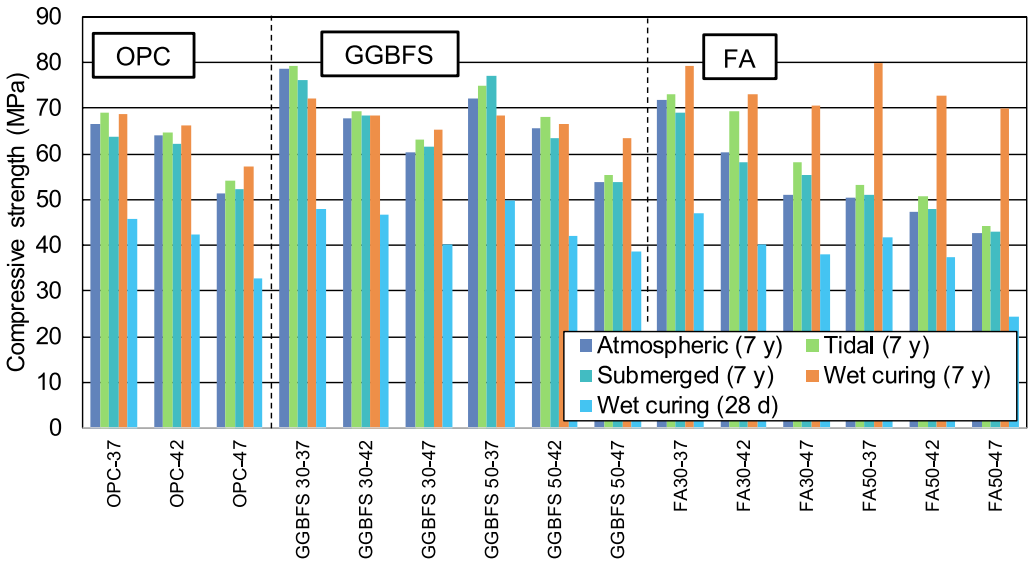

Fig. 4 Compressive strength of concrete exposed to atmospheric, tidal, and submerged conditions over 7 years

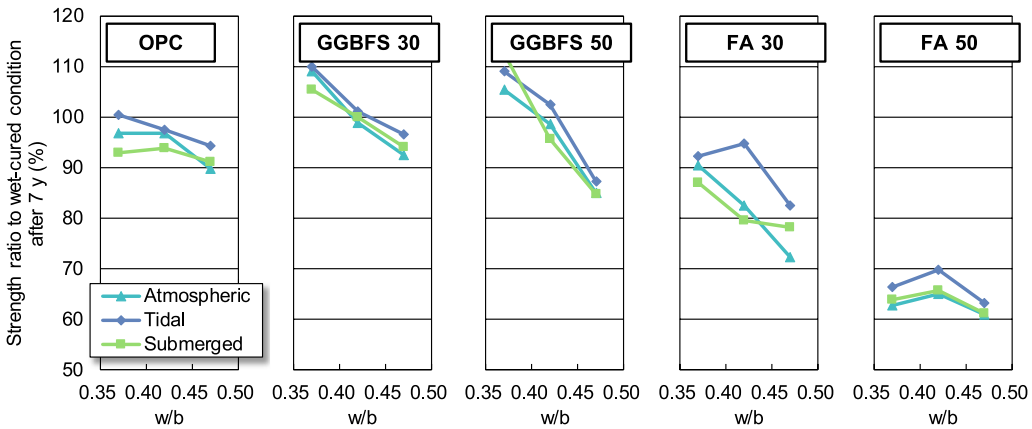

Fig. 5 Relative compressive strength of concrete exposed in sea conditions compared to those with wet curing for 7 years

Additionally, observations from Fig. 5 are as follows: There is an insignificant difference in compressive strength between exposure conditions. In the case of mixtures with 30% and 50% GGBFS, a strength of 90–110% of the standard curing strength is confirmed for all exposure conditions in the w/b range of 0.37–0.47. However, as the FA content gradually increases from 30 to 50%, the strength ratio in Fig. 5 decreases from 70–90% to 60–70%. In other words, OPC and slag cement exhibit a significant advantage in strength development in the marine environment, while high-volume fly ash concrete, on the other hand, has a disadvantage compared to the standard curing condition. It was considered that this effect was induced by the sulfate ions from seawater.

Literature suggests varying effects of fly ash on the chemical reaction of the cement matrix under high-sulfate environments. Some studies report reduced linear expansion caused by sulfate attack, even in continuous exposure to very high concentrations of sulfate (e.g., 10% aqueous solution of Na_2SO_4) (Nie et al., 2015). For instance, Liu et al. (2018) immersed a paste of 40% w/b 0.3 fly ash in 10% Na_2SO_4 water for 3 years, confirming higher strength than OPC 100% after sulfate attack for 3 years and controlled gypsum formation.

However, contrasting results exist; Liu et al. (2012) reported increased ettringite and even gypsum production in high-volume fly ash–cement paste with w/b 0.45 and 25% FA under a high sulfate concentration solution compared to pure cement paste with the same w/b. In the case of GGBFS with a higher calcium concentration than FA, some sulfates were adsorbed to the surface of the C-S-A-H gel without forming a separate crystalline phase, or may produce monosulfate, a more stable phase than ettringite (Kim et al., 2019). Bellmann et al. (2006) also indicated that fly ash contains a large amount of reactive alumina, and binders with an increased alumina content can be more susceptible to the formation of ettringite. Compared to the above research results, this study considered seawater with a much lower sulfate concentration. Also, most studies tested the effect of sulfate on the strength development of fly ash cement within 3 years, whereas this study extended the testing period to 7 years. Therefore, additional experiments on microstructural study are needed to explain the phenomenon in the present work.

Meanwhile, opinions vary regarding the effect of carbonation on concrete strength. While there are reports that the structure becomes denser, and the strength increases with accelerated carbonation in OPC or slag cement concrete (Gruyaert et al., 2013), it was hard to find the reports suggesting strength increases in fly ash concrete.

In terms of structural design, it can be stated that there are no problems with construction as long as the 28-day or maximum 91-day strength is higher than the designed strength. However, high-volume fly ash cement concrete may exhibit strength deviation between the surface exposed to seawater and the interior, necessitating a more careful approach when using it in mass concrete structures.

Fig. 6 presents the models on the strength development of concrete, as outlined in Table 4. As indicated in Table 4, the 28-day compressive strength under standard curing conditions was used as the design strength for the concrete models, denoted as f_{c28}. For all types of models, the calculated strength proved to be conservative compared to the experimental results under various exposure conditions, regardless of binder types.

It is noteworthy that, although the models were initially verified with normal-strength concrete up to one year, they have been successfully applied to predict very-long-term behavior, such as creep, considering several years of duration. The present results indicate that the existing models can be effectively utilized for concrete structures experiencing seawater conditions, even in the long term, up to 7 years, without specific considerations for exposure conditions.

5.2 Neutralization Depth

Fig. 7 illustrates the neutralization depth visualized by spraying a phenolphthalein aqueous solution. The noteworthy finding is that, in most results, the neutralization depth remains consistent regardless of the exposure location. This phenomenon is intriguing, considering that the neutralizing mechanisms in the three conditions are different. As explained in the introduction, the atmospheric exposure condition was expected to be mainly influenced by carbonation, while the submerged zone was neutralized by sulfate (Ganjian & Pouya, 2009). However, the neutralization depth for all specimens was similar, with the variation ranging within 3 mm for all mixtures in Fig. 7.

Mixtures with GGBFS showed similar or even better performance against neutralization compared to OPC 100%. As aforementioned in last section, it is well-known that slag cement has higher resistance against sulfate attack than OPC. Although the microstructure is relatively denser, the slag cement matrix has been known to have a similar carbonation depth compared to the OPC 100% matrix under similar conditions. This is due to a lower calcium hydroxide content in the slag cement matrix, confirming its suitability for durability design. However, in the case of the FA 50 mix, a neutralization depth reached 10–20 mm within just 7 years, depending on the w/b from 0.37 to 0.47. This serves as evidence of

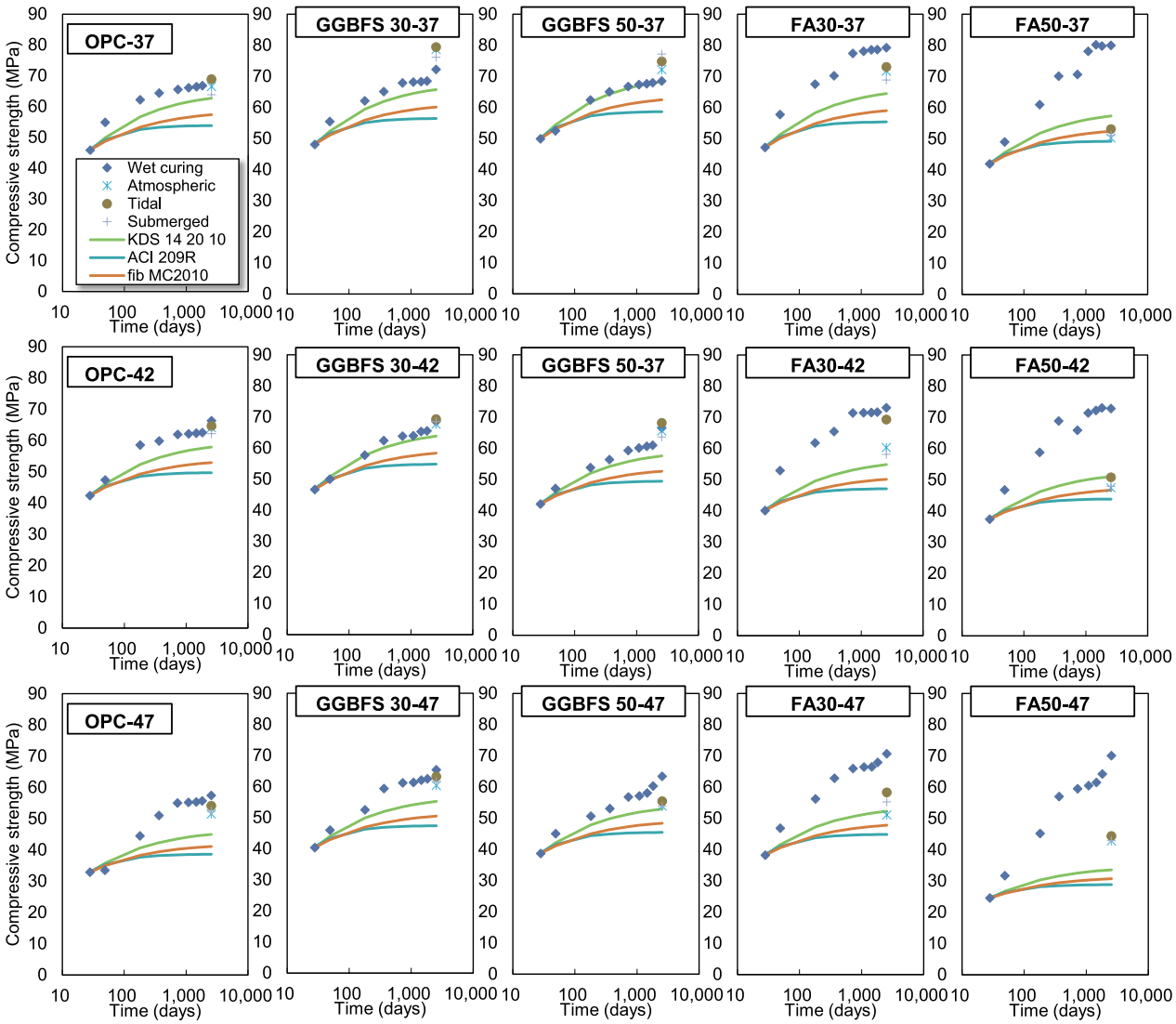

Fig. 6 Comparison of models vs. experimental results for the compressive strength of concrete

a disadvantage of high-volume fly ash in terms of sulfate attack from seawater on concrete.

In Fig. 7, the carbonation depth predicted from the fib Model Code for service life design (MC2010) (Helland, 2013), $y = k\sqrt{t}$, was also plotted. The predicted carbonation depth was adopted to analyze the contribution of carbonation to the neutralization in the cement matrix. The carbonation rate, k in mm/year$^{0.5}$, was obtained considering the exposure condition, and the calculation method is summarized in the Appendix.

In the case of OPC, except for the mixture with w/b 0.37, the neutralization depth obtained through the experiment was deeper than the expected carbonation depth. It should be mentioned that the carbonation depth from the fib MC2010 is for durability-based design, and it may give conservative results compared to actual conditions. Therefore, if the specimens were mainly influenced by carbonation, the neutralization depth from the specimens should be thinner than the predicted carbonation depth (Guiglia & Taliano, 2010). However, as shown in Fig. 7, this was not the case, indicating that the sulfate attack was significant for every exposure condition.

On the other hand, in the case of the mixtures with GGBFS, it can be observed that the neutralization depth from the experiment and designed carbonation depth are almost similar. This implies that slag cement has high resistance against sulfate for all exposure conditions. However, for the mixtures of FA 30 series, the neutralization depth was much deeper than the design carbonation depth under all conditions, regardless of

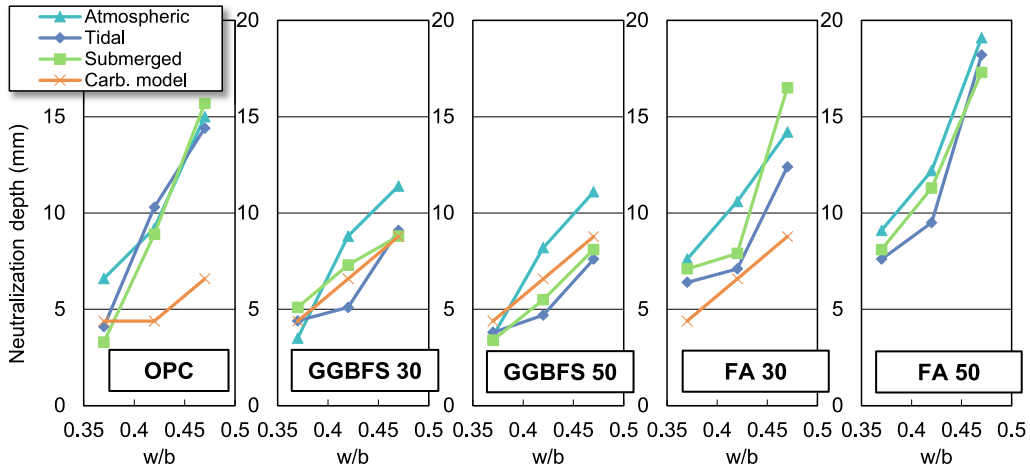

Fig. 7 Comparison of neutralization depth measured by phenolphthalein solution spraying with predicted carbonation depth according to fib MC2010

w/b. It appears that neutralization due to sulfate in seawater has progressed about twice as much in the FA30 mixture than in pure carbonation conditions. Note that the fib MC2010 does not suggest a default carbonation rate value for the FA 50 series (Greve-Dierfeld & Gehlen, 2016a, 2016b).

To summarize the results in this section: in the case of concrete exposed for 7 years, the neutralization depth was consistent across exposure conditions, such as atmospheric, tidal, and submerged zones. Compared to OPC mixes, slag cement has the same or approximately half the neutralization depth depending on w/b. However, when 30–50% of fly ash was used, the neutralization depth was 2–5 mm deeper than that of the OPC mixture. This is a significant difference considering the covering depth.

6 Conclusion

The objective of this investigation was to empirically validate the strength development and neutralization depth of high-performance concrete subjected to 7 years of exposure in the submerged zone, tidal zone, and atmospheric zone along the East coast of South Korea. The study utilized blended cements typically employed in marine concrete structures. Compressive strengths of the concrete under standard curing conditions were compared with those exposed to the marine environment, employing standard models for concrete strength development. Furthermore, the neutralization depth of concrete under the three conditions was gauged using a phenolphthalein solution and juxtaposed with the carbonation depth forecasted from the fib MC2010. The conclusion has been drawn as follows:

1) OPC and slag cement emerge as advantageous in terms of strength development in marine environments, whereas high-volume fly ash concrete may exhibit a disadvantage compared to standard curing conditions. Mixtures with 30% and 50% GGBFS, and 30% FA demonstrated comparable strength at 7 years to OPC 100%, regardless of exposure conditions. The 50% FA mixture displayed higher strength than OPC under standard curing conditions, but this strength did not manifest under external exposure conditions. Despite this, all mixes exhibited a noteworthy increase in compressive strength at 7 years compared to the 28-day period. Caution is warranted when using high-volume fly ash cement concrete in mass concrete structures due to potential strength discrepancies between the surface exposed to seawater and the interior.
2) The results affirm that existing models on compressive strength development can be effectively employed for concrete structures experiencing seawater conditions, even in the long term, up to 7 years, without necessitating specific adjustments for exposure conditions.
3) Regarding concrete exposed for 7 years, the neutralization depth remained consistent across exposure conditions, encompassing atmospheric, tidal, and submerged zones. In comparison to OPC mixes, slag cement exhibited the same or approximately half the neutralization depth, contingent on the w/b. However, in the presence of 30–50% fly ash, the neutralization depth exceeded that of the OPC mixture by 2–5 mm. This discrepancy holds significance, especially when considering the covering depth.

4) It should be noted that the experimental findings in this study may be influenced by the specific w/b and the material properties of the GGBFS and FA used. Therefore, caution should be exercised in generalizing these results across all blended cement systems. Additionally, this study focused solely on compressive strength development and neutralization depth, without incorporating microstructural or chemical analyses. For a more comprehensive understanding of the long-term performance and degradation mechanisms of marine concrete, further research incorporating microstructural characterization and durability-related testing is recommended.

Appendix

Calculation Process of Carbonation Depth from *fib* MC2010 (Greve-Dierfeld & Gehlen, 2016a, 2016b)

The design value of carbonation rate k is calculated with Eq. (1):

$$k = k_{NAC}\sqrt{k_e k_c k_a}W(t), \tag{1}$$

where k_{NAC} is the standard carbonation rate determined in specific test condition (65 ± 5% RH, 20 ± 2 °C, CO2 0.04 ± 0.005 vol.%, 1 atm) (mm/year$^{0.5}$); k_e, k_c, and k_a are subfunctions allowing for the effect of environmental (relative humidity), curing and execution, and CO_2 concentration in the ambient air, respectively, and $W(t)$ is subfunction allowing for the effect of wetting events that will partly inhibit further ingress of CO_2.

The values of k_{NAC} were generally determined by the range of w/b and cement type which assigned to a specific carbonation resistance class (RC) as listed in Table 5.

The values of k_e, k_c, and k_a are determined by following equations:

$$k_e = \left(\frac{1-\left(\frac{RH_a}{100}\right)^f}{1-\left(\frac{RH_l}{100}\right)^f}\right)^g, \tag{2}$$

$$k_c = (t_c/7)^b, \tag{3}$$

$$k_a = C_a/C_l, \tag{4}$$

where, RH_a, and RH_l are relative humidity of the ambient air (%) and reference humidity in laboratory (%); f, g, and b are exponents (-), which generally adopted the values of 2.5, 5, and −0.567, respectively; t_c is curing time (d); C_a and C_l are CO2 concentration of the ambient air and that during testing (kg/m3).

The value of $W(t)$ ranged from 0.2 to 1.0 by weather condition. In the present work, to consider the maximum value carbonation rate for the concrete, the 1.0 of $W(t)$ was adopted.

Acknowledgements

This work was supported by the National Research Foundation of Korea (NRF) grant funded by the Korea government (MSIT) (No. RS-2024-00415881). This research was also supported by Industrial Technology Alchemist Project (No. 20025773, Development of metropolitan Direct Air Capture and Utilization Technologies) funded By the Ministry of Trade, Industry & Energy (MOTIE, Korea).

Author contributions

Hyeong-Ki Kim: Validation, writing—original draft, visualization. Jong-Suk Lee: Conceptualization, methodology, resources, supervision, project administration, funding acquisition. Hyeon-Woo Lee: Formal analysis, data curation. Seung-Jun Kwon: Conceptualization, methodology, writing—review and editing, supervision, project administration, funding acquisition.

Funding

National Research Foundation of Korea (NRF) (No. NRF-2020R1A2C2009462) and MOTIE (No. 20025773).

Availability of data and materials

All the datasets associated with this study are available from the corresponding author upon request.

Table 5 Ranges of water-to-cement ratio depending on cement type assigned to a specific carbonation resistance class (RC)

Class	RC2	RC3	RC4	RC5	RC6	RC7
Range of k_{NAC} (mm/year0.5)	1–2	2–3	2–4	4–5	5–6	6–7
Cement type	w/b					
CEM I	0.45	0.50	0.55	0.60	0.65	-
CEM II/A	0.45	0.50	0.55	0.60	0.65	-
CEM II/B	0.40	0.45	0.50	0.55	0.60	0.65
CEM III/A	0.40	0.45	0.50	0.55	0.60	0.65
CEM III/B	–	0.40	0.45	0.50	0.55	0.60

Refer to EN 197-1 on type of cement (CEM series)

Declarations

Ethics approval and consent to participate
All authors of the manuscript confirm the ethics approval and consent to participate following the Journal's policies.

Competing interests
The authors declare no conflict of interest.

Author details
[1]Department of Architectural Engineering, Chosun University, 309, Pilmun-Daero, Dong-gu, Gwangju 61452, Republic of Korea. [2]Department of Structural Engineering Research, Korea Institute of Civil Engineering and Building Technology, 283 Goyang-daero, Insanseo-gu, Goyang 10233, Republic of Korea. [3]Department of Civil and Environmental Engineering, Hannam University, Hannamro 70, Daejoen 34430, Republic of Korea.

Received: 24 January 2024 Accepted: 18 March 2025
Published online: 01 June 2025

References

Alemu, A. S., Lee, B. Y., Park, S., & Kim, H.-K. (2022). Self-healing of Portland and slag cement binder systems incorporating circulating fluidized bed combustion bottom ash. *Construction and Building Materials, 314*, 125571.
Al-Khaiat, H., & Fattuhi, N. (2001). Long-term strength development of concrete in arid conditions. *Cement and Concrete Composites, 23*(4–5), 363–373.
Bellmann, F., Möser, B., & Stark, J. (2006). Influence of sulfate solution concentration on the formation of gypsum in sulfate resistance test specimen. *Cement and Concrete Research, 36*(2), 358–363.
Chidiac, S. E., Moutassem, F., & Mahmoodzadeh, F. (2013). Compressive strength model for concrete. *Magazine of Concrete Research, 65*(9), 557–572.
De Weerdt, K., Justnes, H., & Geiker, M. R. (2014). Changes in the phase assemblage of concrete exposed to sea water. *Cement and Concrete Composites, 47*, 53–63.
Escalante, J., Gomez, L., Johal, K., Mendoza, G., Mancha, H., & Mendez, J. (2001). Reactivity of blast-furnace slag in Portland cement blends hydrated under different conditions. *Cement and Concrete Research, 31*(10), 1403–1409.
Ganjian, E., & Pouya, H. S. (2009). The effect of Persian Gulf tidal zone exposure on durability of mixes containing silica fume and blast furnace slag. *Construction and Building Materials, 23*(2), 644–652.
Gruyaert, E., Van den Heede, P., & De Belie, N. (2013). Carbonation of slag concrete: Effect of the cement replacement level and curing on the carbonation coefficient – Effect of carbonation on the pore structure. *Cement and Concrete Composites, 35*(1), 39–48.
Guiglia, M., & Taliano, M. (2013). Comparison of carbonation depths measured on in-field exposed existing r.c. structures with predictions made using fib-Model Code 2010. *Cement and Concrete Composites, 38*, 92–108.
Helland, S. (2013). Design for service life: Implementation of fib Model Code 2010 rules in the operational code ISO 16204. *Structural Concrete, 14*(1), 10–18.
Hwang, K., Noguchi, T., & Tomosawa, F. (2004). Prediction model of compressive strength development of fly-ash concrete. *Cement and Concrete Research, 34*(12), 2269–2276.
Jang, S.-Y., Karthick, S., & Kwon, S.-J. (2017). Investigation on durability performance in early aged high-performance concrete containing GGBFS and FA. *Advances in Materials Science and Engineering, 2017*, 1–11.
Kim, D.-M., Yun, S.-T., Kwon, M. J., Mayer, B., & Kim, K.-H. (2014). Assessing redox zones and seawater intrusion in a coastal aquifer in South Korea using hydrogeological, chemical and isotopic approaches. *Chemical Geology, 390*, 119–134.
Kim, H.-J., Tafesse, M., Lee, H. K., & Kim, H.-K. (2019). Incorporation of CFBC ash in sodium silicate-activated slag system: Modification of microstructures and its effect on shrinkage. *Cement and Concrete Research, 123*, 105771.
Kim, J.-K., Moon, Y.-H., & Eo, S.-H. (1998). Compressive strength development of concrete with different curing time and temperature. *Cement and Concrete Research, 28*(12), 1761–1773.
Kwon, S.-J., & Na, U.-J. (2011). Prediction of durability for RC columns with crack and joint under carbonation based on probabilistic approach. *International Journal of Concrete Structures and Materials, 5*(1), 11–18.
Lee, C., Lee, S., & Nguyen, N. (2016). Modeling of compressive strength development of high-early-strength-concrete at different curing temperatures. *International Journal of Concrete Structures and Materials, 10*, 205–219.
Liu, K., Sun, D., Wang, A., Zhang, G., & Tang, J. (2018). Long-term performance of blended cement paste containing fly ash against sodium sulfate attack. *Journal of Materials in Civil Engineering, 30*(12), 04018309.
Liu, Q., Sun, L., Zhu, X., Xu, L., & Zhao, G. (2022). Chloride transport in the reinforced concrete column under the marine environment: Distinguish the atmospheric, tidal-splash and submerged zones. *Structures, 39*, 365–377.
Liu, Z., Deng, D., De Schutter, G., & Yu, Z. (2012). Chemical sulfate attack performance of partially exposed cement and cement+ fly ash paste. *Construction and Building Materials, 28*(1), 230–237.
Mehta, P. K., & Haynes, H. H. (1975). Durability of concrete in seawater. *Journal of the Structural Division, 101*(8), 1679–1686.
Müller, H. S., Anders, I., Breiner, R., & Vogel, M. (2013). Concrete: Treatment of types and properties in fib Model Code 2010. *Structural Concrete, 14*(4), 320–334.
Mun, J.-S., Yang, K.-H., & Jeon, Y.-S. (2014). Maturity-based model for concrete compressive strength with different supplementary cementitious materials. *Journal of the Korea Institute for Structural Maintenance and Inspection, 18*(6), 82–89.
Nie, Q., Zhou, C., Li, H., Shu, X., Gong, H., & Huang, B. (2015). Numerical simulation of fly ash concrete under sulfate attack. *Construction and Building Materials, 84*, 261–268.
Park, H.-G., Hwang, H.-J., Hong, G.-H., Kim, Y.-N., & Kim, J.-Y. (2012). Immediate and long-term deflections of reinforced concrete slabs affected by early-age loading and low temperature. *ACI Structural Journal, 109*(3), 413–422.
Ragab, A. M., Elgammal, M. A., Hodhod, O. A., & Ahmed, T. E. (2016). Evaluation of field concrete deterioration under real conditions of seawater attack. *Construction and Building Materials, 119*, 130–144.
Saeki, T. (1991). Mechanism of carbonation and prediction of carbonation process of concrete. *Concrete Library International of JSCE, 17*, 23–36.
Thomas, M., & Matthews, J. (2004). Performance of pfa concrete in a marine environment—10-year results. *Cement and Concrete Composites, 26*(1), 5–20.
von Greve-Dierfeld, S., & Gehlen, C. (2016a). Performance-based durability design, carbonation part 2 – Classification of concrete. *Structural Concrete, 17*(4), 523–532.
von Greve-Dierfeld, S., & Gehlen, C. (2016b). Performance based durability design, carbonation part 1 – Benchmarking of European present design rules. *Structural Concrete, 17*(3), 309–328.
Wang, X.-Y., & Park, K.-B. (2015). Analysis of compressive strength development of concrete containing high volume fly ash. *Construction and Building Materials, 98*, 810–819.
Washa, G. W., Saemann, J. C., & Cramer, S. M. (1989). Fifty-year properties of concrete made in 1937. *Materials Journal, 86*(4), 367–371.
Washa, G. W., & Wendt, K.F. (1975). *Fifty year properties of concrete*. In *Journal Proceedings*..
Whittaker, M. J. (2014). *The impact of slag composition on the microstructure of composite slag cements exposed to sulfate attack*. University of Leeds.
Zhu, X., Zi, G., Cao, Z., & Cheng, X. (2016). Combined effect of carbonation and chloride ingress in concrete. *Construction and Building Materials, 110*, 369–380.

Publisher's Note

Hyeong-Ki Kim Professor, Department of Architectural Engineering, Chosun University.

Jong-Suk Lee Research Fellow, Department of Structural Engineering Research, Korea Institute of Civil Engineering and Building Technology.

Hyeon-Woo Lee Graduate student, Department of Civil and Environmental Engineering, Hannam University.

Seung-Jun Kwon Professor, Department of Civil and Environmental Engineering, Hannam University.